ECCOMAS Congress 2016
VII European Congress on Computational Methods in Applied Sciences and Engineering
M. Papadrakakis, V. Papadopoulos, G. Stefanou, V. Plevris (eds.)
Crete Island, Greece, 5–10 June 2016

A LARGE TIME STEP ROE SCHEME APPLIED TO TWO-PHASE FLOW

Sofia Lindqvist[1,2] **and Halvor Lund**[2,3]

[1]Mathematical Institute, University of Oxford, Andrew Wiles Building, Woodstock Rd, Oxford OX2 6GG, UK.
[2]SINTEF Energy Research, P. O. Box 4761 Sluppen, NO-7465 Trondheim, Norway.
[3]Corresponding author, e-mail: halvor.lund@sintef.no

Keywords: Large time step, Roe scheme, two-phase flow

Abstract. *We consider a large time step (LTS) Roe scheme, originally suggested by LeVeque [*Comm. Pure Appl. Math.*, 37 (1984), pp. 463–477] which has attained increased popularity in recent years. The scheme is based on a wave formulation of the ordinary Roe scheme, and the assumption that waves interact linearly. This assumption lets us propagate waves over more than one cell, thereby violating the ordinary CFL condition requiring the Courant number to be less than one. The LTS Roe scheme is applied to a two-phase flow model with phase transfer, modelled using the stiffened-gas equation of state. Results from various test cases show that the LTS Roe scheme with moderate Courant numbers is significantly more efficient than the ordinary Roe scheme, measured by an error-to-runtime ratio. The optimal Courant number is mainly a trade-off between reduced runtime due to fewer time steps, and increased error due to the assumption of linear wave interactions.*

1 INTRODUCTION

The motivation for our paper is solving hyperbolic conservation laws of the form

$$\boldsymbol{u}_t + \boldsymbol{f}(\boldsymbol{u})_x = 0, \tag{1a}$$

$$\boldsymbol{u}(x, 0) = \boldsymbol{u}_0(x). \tag{1b}$$

Here $\boldsymbol{u} \in \mathbb{R}^N$ is a vector of N unknowns, $\boldsymbol{f} : \mathbb{R}^N \to \mathbb{R}^N$ is a hyperbolic flux function, and $\boldsymbol{u}_0$ some initial condition. Numerical methods for solving such problems often fit into the finite volume framework, which solves eq. (1) in the integral form,

$$\frac{\mathrm{d}}{\mathrm{d}t}\boldsymbol{U}_i = \frac{\boldsymbol{F}_{i-1/2} - \boldsymbol{F}_{i+1/2}}{\Delta x}, \tag{2}$$

where $\boldsymbol{U}_i$ approximates the average of $\boldsymbol{u}$ over volume i. The numerical flux function $\boldsymbol{F}_{i-1/2}$ approximates the flux between cells $i-1$ and i, using only the cell averages $\{\boldsymbol{U}_i\}$.

Standard explicit finite volume methods typically use a three-point stencil which limits the time steps to prevent waves from travelling more than one cell. Large time step (LTS) schemes seek to circumvent this restriction by using a larger stencil, to allow longer time steps and therefore more efficient numerical simulations. Explicit LTS schemes also have the advantage of being easily parallelizable, in contrast to implicit schemes, as pointed out by e.g. Norman et al. [20]. One of the first large time step schemes for scalar conservation laws was presented by LeVeque [9] in 1982. This scheme represents all waves as shocks, and handles the merging of shocks explicitly. LeVeque later introduced an LTS scheme for systems of conservation laws [11] using an exact Riemann solver, and proposed one using the Roe approximate Riemann solver [10]. The wave interactions are assumed to be linear, which removes the need to handle wave interactions explicitly. More recently, Qian and Lee [21] extended this scheme by taking wave interactions into account. Norman et al. [20] developed a LTS scheme similar to LeVeque's approach, based on a WENO discretization.

Harten [4] developed a class of LTS schemes of second order with $2K + 3$ stencils, where K is the Courant number. He proves that the scheme is total-variation diminishing (TVD) for linearized systems, and introduces an entropy fix. This scheme was later picked up by Qian and Lee [22] and slightly modified to improve its stability. They also constructed an LTS scheme for Yee's upwind TVD scheme [27]. Other approaches to LTS schemes outside the framework of Godunov methods have also been presented, such as the front-tracking scheme of Holden et al. [6].

Murillo et al. [19] and Morales-Hernández et al. [17] picked up on LeVeque's ideas and applied an LTS Roe scheme to the shallow water equations. Recently, Thompson and Moeller [26] introduced their wave-in-cell numerical scheme for hyperbolic conservation laws. The scheme has many similarities with front-tracking schemes, and tracks the waves from each Riemann problem explicitly, assuming they interact linearly. For nonlinear systems, the solution is projected onto a grid after each time step. Both these schemes are equivalent to the LTS Roe scheme we present in this paper, although applied to a different system of equations.

The LTS Roe scheme presented in the current paper is built on the general framework of TVD LTS schemes described by Lindqvist et al. [13]. This work derived TVD requirements for a class of LTS schemes, and discusses how existing schemes like LTS Godunov and LTS Roe fit into this TVD LTS framework. They prove that an LTS extension of the Lax-Friedrichs scheme is the most diffusive scheme, and that the LTS Roe scheme is the least diffusive scheme.

In this paper, we apply the LTS Roe scheme to a two-phase flow model for CO_2 pipelines, with thermodynamics described by the stiffened-gas equation of state. CO_2 capture and storage (CCS) is expected to play a crucial role in reducing the world's emissions of greenhouse gases. In the International Energy Agency's two-degree scenario (2DS), CCS will contribute to reducing the global CO_2 emissions by about seven gigatonnes per year in 2050 [7]. CO_2 pipelines will be one of the key elements in a CCS infrastructure, and accurate models and efficient numerical methods are necessary to predict their operation.

1.1 Paper outline

Our paper is organized as follows: In section 2, we give a short introduction to the ordinary Roe scheme and its large time step (LTS) extension. Section 3 describes the homogeneous equilibrium model for two-phase flow, which we will use in our numerical test cases. The model is applied to two-phase flow of CO_2, the thermodynamics of which is described by the stiffened-gas equation of state. Results from various test cases relevant to compressible two-phase flow are presented in section 4, where we investigate how the LTS Roe scheme performs for Courant numbers greater than 1. The different Courant numbers are compared in terms of error versus runtime. Finally, section 5 summarizes our findings and outlines how the scheme can be improved and extended to higher order.

2 NUMERICAL SCHEME

To solve the hyperbolic equation system (1) numerically, we divide the x and t axes into finite volumes of size $(\Delta x, \Delta t)$, and integrate over one such cell,

$$\boldsymbol{U}_i^{n+1} = \boldsymbol{U}_i^n + \frac{\Delta t}{\Delta x}(\boldsymbol{F}_{i-1/2}^n - \boldsymbol{F}_{i+1/2}^n), \tag{3}$$

where $\boldsymbol{U}_i^n$ is the average of $\boldsymbol{u}$ over cell i at time t^n, and $\boldsymbol{F}_{i-1/2}^n$ approximates the flux at the cell interface between cells $i-1$ and i.

In the classical Roe scheme [24], the numerical flux $\boldsymbol{F}_{i-1/2}^n$ is given by

$$\boldsymbol{F}_{i-1/2}^n = \frac{1}{2}(\boldsymbol{F}(\boldsymbol{U}_i^n) + \boldsymbol{F}(\boldsymbol{U}_{i-1}^n)) - \frac{1}{2}|\hat{\boldsymbol{A}}(\boldsymbol{U}_{i-1}^n, \boldsymbol{U}_i^n)|(\boldsymbol{U}_i^n - \boldsymbol{U}_{i-1}^n), \tag{4}$$

where $\hat{\boldsymbol{A}}$ is the Roe matrix, which must satisfy three properties:

1. Conserving: $\hat{\boldsymbol{A}}(\boldsymbol{U}_\mathrm{L}, \boldsymbol{U}_\mathrm{R})(\boldsymbol{U}_\mathrm{R} - \boldsymbol{U}_\mathrm{L}) = \boldsymbol{F}(\boldsymbol{U}_\mathrm{R}) - \boldsymbol{F}(\boldsymbol{U}_\mathrm{L})$
2. Hyperbolic: $\hat{\boldsymbol{A}}(\boldsymbol{U}_\mathrm{L}, \boldsymbol{U}_\mathrm{R})$ is diagonalizable with real eigenvalues
3. Consistent: $\hat{\boldsymbol{A}}(\boldsymbol{U}_\mathrm{L}, \boldsymbol{U}_\mathrm{R}) \to \frac{\partial \boldsymbol{F}}{\partial \boldsymbol{U}}$ smoothly as $\boldsymbol{U}_\mathrm{L}, \boldsymbol{U}_\mathrm{R} \to \boldsymbol{U}$

Here, $\boldsymbol{U}_\mathrm{L}$/$\boldsymbol{U}_\mathrm{R}$ are the states to the immediate left/right of the cell interface.

If $\hat{\boldsymbol{A}} = \hat{\boldsymbol{R}}\hat{\boldsymbol{\Lambda}}\hat{\boldsymbol{R}}^{-1}$ is a diagonalization of the Roe matrix, the absolute Roe matrix is $|\hat{\boldsymbol{A}}| = \hat{\boldsymbol{R}}|\hat{\boldsymbol{\Lambda}}|\hat{\boldsymbol{R}}^{-1}$. Here $|\hat{\boldsymbol{\Lambda}}| = \mathrm{diag}(|\hat{\lambda}_1|, \ldots, |\hat{\lambda}_N|)$ is the diagonal matrix with the absolute eigenvalues of $\hat{\boldsymbol{A}}$. It is instructive for our further derivations to rewrite the scheme in terms of waves, as

$$\boldsymbol{U}_i^{n+1} = \boldsymbol{U}_i^n - \frac{\Delta t}{\Delta x}(\hat{\boldsymbol{A}}_{i-1/2}^+ \Delta_{i-1/2} + \hat{\boldsymbol{A}}_{i+1/2}^- \Delta_{i+1/2}), \tag{5}$$

where $\Delta_{i-1/2} = \boldsymbol{U}_i - \boldsymbol{U}_{i-1}$, $\hat{\boldsymbol{A}}^\pm = \hat{\boldsymbol{R}}\hat{\boldsymbol{\Lambda}}^\pm\hat{\boldsymbol{R}}^{-1}$, and $\hat{\boldsymbol{\Lambda}}^\pm = \pm\mathrm{diag}(\max(\pm\hat{\lambda}_1, 0), \ldots, \max(\pm\hat{\lambda}_N, 0))$. This formulation illustrates how the fluctuations $\hat{\boldsymbol{A}}_{i-1/2}^+ \Delta_{i-1/2}$ (right-going) and $\hat{\boldsymbol{A}}_{i+1/2}^- \Delta_{i+1/2}$ (left-going) propagate as waves in each direction.

2.1 Large time step (LTS) Roe scheme

In this section, we present the most important aspects of the LTS Roe scheme, which was first proposed by Leveque [10]. For more details, the reader is referred to Lindqvist et al. [13]. The time step Δt in the ordinary Roe scheme in eq. (5) is limited by the CFL condition [2], which requires the Courant number $\mathcal{C}$ to be less than one,

$$\mathcal{C} = \frac{\Delta t}{\Delta x} \max_{k,i}(|\lambda_{k,i}|) < 1. \tag{6}$$

Here $\lambda_{k,i}$ is the kth eigenvalue of $\partial \boldsymbol{F}/\partial \boldsymbol{U}$ in the ith cell. This condition ensures that no waves travel more than one cell in a single time step, or equivalently that the numerical domain of dependence includes the mathematical domain of dependence. The motivation behind the LTS Roe scheme (or any LTS scheme, for that matter) is to enable larger time steps by extending the numerical domain of dependence.

If we assume that all wave interactions are linear, a natural extension of the Roe scheme is

$$\boldsymbol{U}_j^{n+1} = \boldsymbol{U}_j^n - \frac{\Delta t}{\Delta x} \sum_{i=0}^{\infty} \left(\hat{\boldsymbol{A}}^{i+}_{j-1/2-i} \Delta_{j-1/2-i} + \hat{\boldsymbol{A}}^{i-}_{j+1/2+i} \Delta_{j+1/2+i} \right), \tag{7}$$

where

$$\hat{\boldsymbol{A}}^{i\pm} = \hat{\boldsymbol{R}} \hat{\boldsymbol{\Lambda}}^{i\pm} \hat{\boldsymbol{R}}^{-1}, \tag{8a}$$

$$\hat{\boldsymbol{\Lambda}}^{i\pm} = \text{diag}(\hat{\lambda}^{i\pm}), \tag{8b}$$

$$\hat{\lambda}^{i+} = \max\left(0, \min\left(\hat{\lambda} - i\frac{\Delta x}{\Delta t}, \frac{\Delta x}{\Delta t}\right)\right), \tag{8c}$$

$$\hat{\lambda}^{i-} = \min\left(0, \max\left(\hat{\lambda} + i\frac{\Delta x}{\Delta t}, -\frac{\Delta x}{\Delta t}\right)\right). \tag{8d}$$

Although the sum in eq. (7) appears to be infinite, $\hat{\boldsymbol{A}}^{i\pm}$ will be zero for sufficiently large i. This reduces to the ordinary Roe scheme for Courant numbers less than 1. More importantly, it allows arbitrarily large Courant numbers while still respecting the condition that the numerical domain of dependence include the mathematical one. For scalar equations, we also know that the scheme is TVD [13]. For a Courant number of $\mathcal{C}$, the scheme's stencil will include a maximum of $2\lceil \mathcal{C} \rceil + 1$ cells.

2.2 Entropy fix

Lindqvist et al. [13] show that the scheme is unconditionally total-variation diminishing for scalar equations for all Courant numbers. From the Lax-Wendroff theorem [8] we know that TVD schemes converge to a weak solution for scalar equations, but not necessarily the correct entropy solution [5]. In [13], it is suggested to vary the time step slightly, which ensures that entropy-violating shocks are eliminated. In this work, we employ this entropy fix, by using a modified Courant number $\hat{C}$ given by

$$\hat{C} = \mathcal{C} - r, \tag{9}$$

where r is sampled randomly and uniformly from the interval $(0, 1)$.

Lindqvist et al. [13] also prove an extension of Harten's lemma [3]: All unconditionally TVD schemes have numerical viscosities that are bounded by the LTS Lax-Friedrichs and the LTS Roe schemes. The related work of Qui and Shu [23] also concerns the entropy properties of TVD LTS schemes.

3 TWO-PHASE FLOW MODEL

For our numerical test cases, we model the two-phase (gas-liquid) flow of CO_2 using the one-dimensional homogeneous equilibrium model (HEM) [25], in which the two phases have the same pressure, temperature, chemical potential and velocity. The advantage of this model is that it does not require explicit modelling of the interaction between the phases, such as interfacial friction, heat and mass. It can nevertheless describe two-phase flow reasonably well in cases where the two phases are tightly coupled, such as in bubbly flow or in small diameter pipes. This model has been used for simulation of two-phase flow by e.g. Clerc [1], Lund et al. [14].

The homogeneous equilibrium model can be expressed using the Euler equations,

$$\frac{\partial \rho}{\partial t} + \frac{\partial (\rho v)}{\partial x} = 0, \tag{10a}$$

$$\frac{\partial \rho v}{\partial t} + \frac{\partial (\rho v^2 + p)}{\partial x} = 0, \tag{10b}$$

$$\frac{\partial E}{\partial t} + \frac{\partial [v(E+p)]}{\partial x} = 0, \tag{10c}$$

where ρ is the mixture density, v is the velocity, p is the pressure and E is the mixture energy density. The latter can be expressed as

$$E = \rho \left(e + \frac{1}{2} v^2 \right), \tag{11}$$

where e is the mixture internal energy density.

To close the equation system (10), we need an equation of state (EOS) to relate the pressure p to the mixture density ρ and the mixture internal energy density e. In this work, we construct a mixture EOS by describing each phase using the stiffened-gas EOS, as described by e.g. Menikoff [15], Menikoff and Plohr [16]. For each phase, this can be viewed as a linearization of a reference EOS, and has the advantage of being simple and highly efficient, while still giving relatively accurate results close to a chosen reference point. The two stiffened-gas equations of state are combined into a mixture EOS by requiring that both phases have the same pressure, temperature and chemical potential.

The pressure, internal energy and chemical potential (for each phase) are given by

$$p_k(\rho_k, T) = \rho_k(\gamma_k - 1) c_{v,k} T - p_{\infty,k}, \tag{12}$$

$$e_k(\rho_k, T) = c_{v,k} T + \frac{p_{\infty,k}}{\rho_k} + e_{*,k}, \tag{13}$$

$$\mu_k(\rho_k, T) = \gamma_k c_{v,k} T + e_{*,k} - c_{v,k} T \ln \left(\frac{T}{T_{0,k}} \left(\frac{\rho_{0,k}}{\rho} \right)^{\gamma_k - 1} \right) - s_{0,k} T, \tag{14}$$

where γ_k, $c_{v,k}$, $p_{\infty,k}$, $e_{*,k}$, $T_{0,k}$, $\rho_{0,k}$ and $s_{0,k}$ are parameters specific for phase $k = \{\mathrm{g}, \ell\}$ where g denotes gas and ℓ denotes liquid. These parameters can be fitted using experimental data or a reference EOS for a given fluid.

The pressure p must be expressed as a function of mixture density $\rho \equiv \alpha_\mathrm{g}\rho_\mathrm{g} + \alpha_\ell\rho_\ell$ and mixture energy $e \equiv (\alpha_\mathrm{g}\rho_\mathrm{g}e_\mathrm{g} + \alpha_\ell\rho_\ell e_\ell)/\rho$, with the condition that the phase pressures, temperatures and chemical potentials be equal, $p_\mathrm{g} = p_\ell = p$, $T_\mathrm{g} = T_\ell = T$ and $\mu_\mathrm{g} = \mu_\ell$. This leads to a transcendental equation system that is solved numerically using a Newton method, as in Lund et al. [14].

In the LTS Roe scheme for the homogeneous equilibrium model (10), we use the Roe matrix described by Morin et al. [18]. The Roe matrix is diagonalized numerically.

4 RESULTS

In this section, we will present results from various test cases relevant to compressible flow. We will compare the LTS Roe scheme to an ordinary Roe scheme with a Courant number less than one. The performance of the two methods will be measured by the error achieved for a certain runtime, which in this case is more relevant than the error on a certain grid, as long as we are not limited by memory. The error is measured in the L^2 norm by comparing the numerical solutions to reference solutions calculated with a Roe method with minmod flux limiter on a 6000 cell grid. More precisely, the error $\mathcal{E}$ can be expressed as

$$\mathcal{E} = \frac{\sqrt{\sum_{i=1}^{n}(U_i - U_{\mathrm{ref},i})^2}}{n}, \tag{15}$$

where U_i and $U_{\mathrm{ref},i}$ are the numerical and the reference solution at point i, respectively.

The properties used for the stiffened gas equation of state are listed in table 1. These properties are fitted to match the real properties of carbon dioxide at $p = 45\,\mathrm{bar}$ and saturation conditions ($T = 283.13\,\mathrm{K}$).

Table 1: Stiffened gas parameters, fitted to CO_2 at $45\,\mathrm{bar}$ and saturation conditions.

Symbol	Unit	Gas value	Liquid value
γ	–	1.06	1.23
p_∞	Pa	8.86×10^5	1.32×10^8
c_v	$\mathrm{J/(kg\,K)}$	2411	2436
e_*	$\mathrm{J/kg}$	-3.00×10^5	-6.23×10^5
T_0	K	283.13	283.13
ρ_0	$\mathrm{kg/m^3}$	135	861.27
s_0	$\mathrm{J/(kg\,K)}$	1784	1088

4.1 Advected volume fraction discontinuity

In this case, there is an initial discontinuity in the volume fraction which is advected in the positive x direction at a constant speed. The initial conditions are

$$p = 20\,\mathrm{bar}, \tag{16a}$$

$$u = 10\,\mathrm{m/s}, \tag{16b}$$

$$\alpha_\ell = \begin{cases} 0.1 \text{ if } x \leq 2500\,\mathrm{m}, \\ 0.9 \text{ if } x > 2500\,\mathrm{m}, \end{cases} \tag{16c}$$

$$T = T_\mathrm{eq}(p), \tag{16d}$$

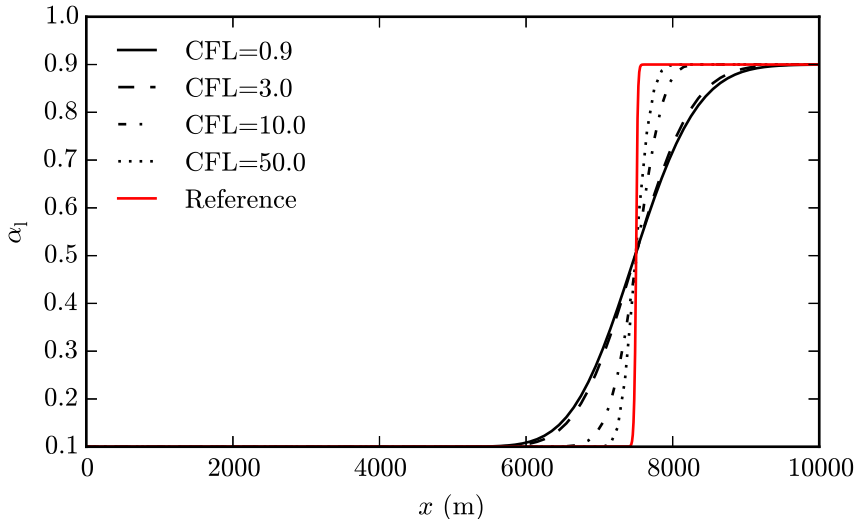

Figure 1: Liquid volume fraction discontinuity at time $t = 500\,\mathrm{s}$ on a grid with 100 cells for initial conditions given in eq. (16).

where $T_{\mathrm{eq}}(p)$ denotes the equilibrium (boiling) temperature at the pressure p.

Figure 1 shows the liquid volume fraction at time $t = 500\,\mathrm{s}$ for four different Courant numbers, compared to the reference solution. Since each time step introduces some diffusion, the LTS Roe scheme has a significant advantage over the ordinary Roe scheme for this case. As an example, Roe with $\mathcal{C} = 0.9$ will need roughly 56 times more time steps than LTS Roe with $\mathcal{C} = 50$, leading to more diffusion and a less accurate solution. In addition, fewer time steps means a shorter computational time, which adds to the advantages of using LTS Roe for this case. This seems to indicate that it is beneficial to increase the Courant number indefinitely, however this is not the case for all initial conditions, as we will see in the following sections.

4.2 Rarefaction and shock

This case starts with a discontinuity in both volume fraction and pressure, which leads to both a rarefaction wave and a shock wave. The initial condition is given by

$$u = 0, \tag{17a}$$

$$\alpha_\ell = \begin{cases} 0.1 & \text{if } x < 5000\,\mathrm{m}, \\ 0.9 & \text{if } x > 5000\,\mathrm{m}, \end{cases} \tag{17b}$$

$$p = \begin{cases} 20\,\mathrm{bar} & \text{if } x < 5000\,\mathrm{m}, \\ 60\,\mathrm{bar} & \text{if } x > 5000\,\mathrm{m}, \end{cases} \tag{17c}$$

$$T = T_{\mathrm{eq}}(p). \tag{17d}$$

Figures 2 and 3 show the pressure and liquid volume fraction, respectively, at $t = 25\,\mathrm{s}$. In this case, it is clear that a Courant number of 50 is far too high, and also $\mathcal{C} = 10.0$ leads to some oscillations. $\mathcal{C} = 3.0$ seems more appropriate and gives a solution similar to that achieved with $\mathcal{C} = 0.9$, although some oscillations are present. However, since $\mathcal{C} = 0.9$ requires about 3 times as many time steps, $\mathcal{C} = 3.0$ might well be the most appropriate choice when it comes to runtime per error.

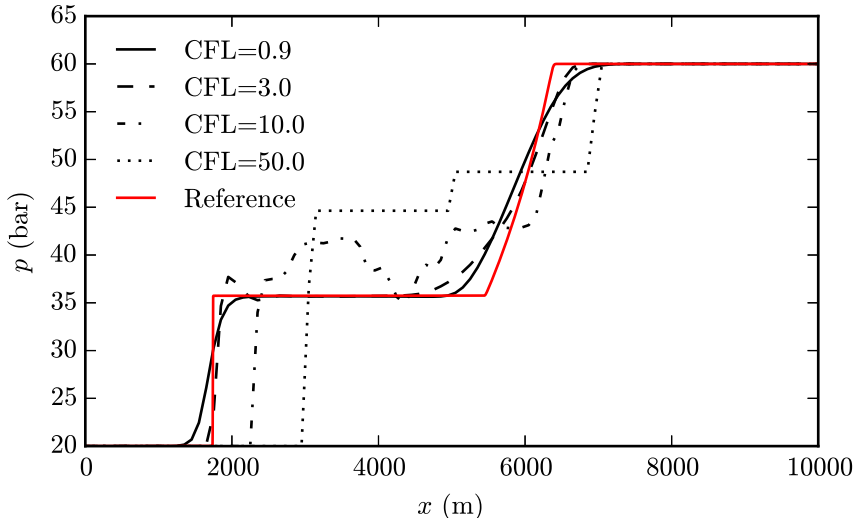

Figure 2: Pressure for at time $t = 25\,\mathrm{s}$ on a grid with 100 cells for initial conditions given in eq. (17).

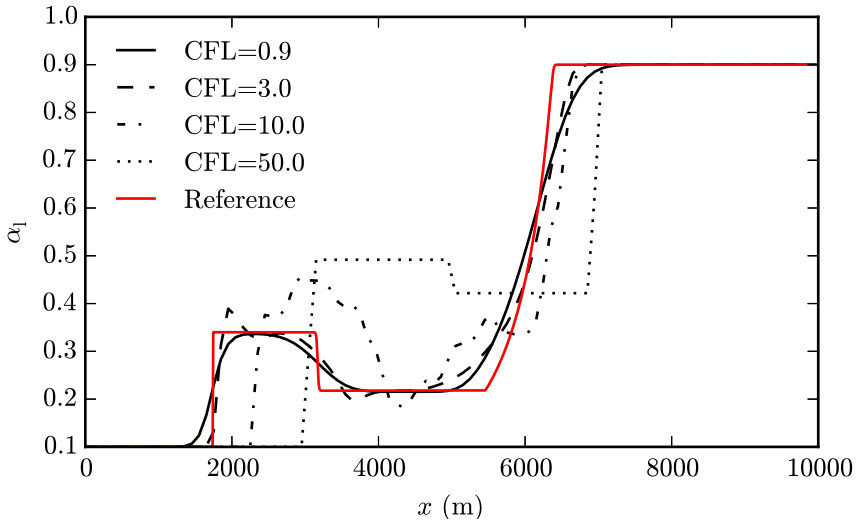

Figure 3: Pressure for at time $t = 25\,\mathrm{s}$ on a grid with 100 cells for initial conditions given in eq. (17).

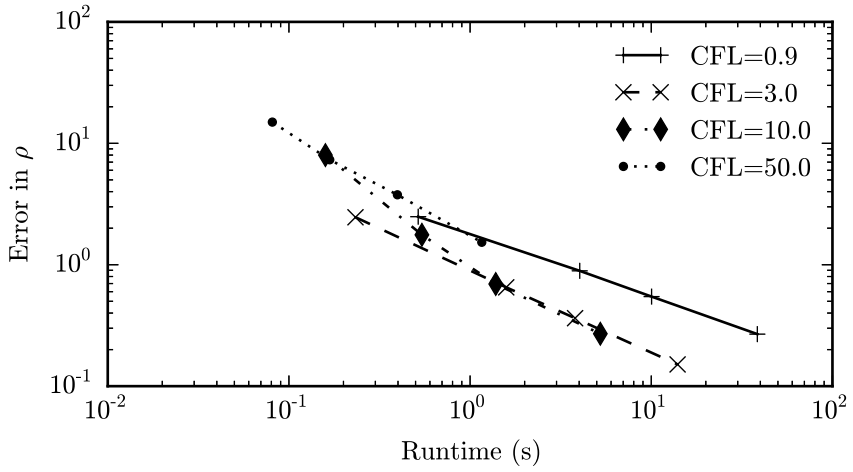

(a) Error in ρ.

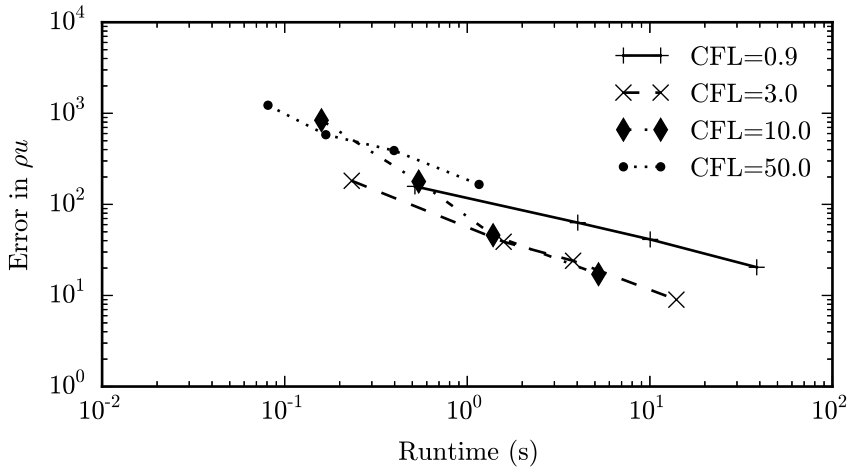

(b) Error in ρu.

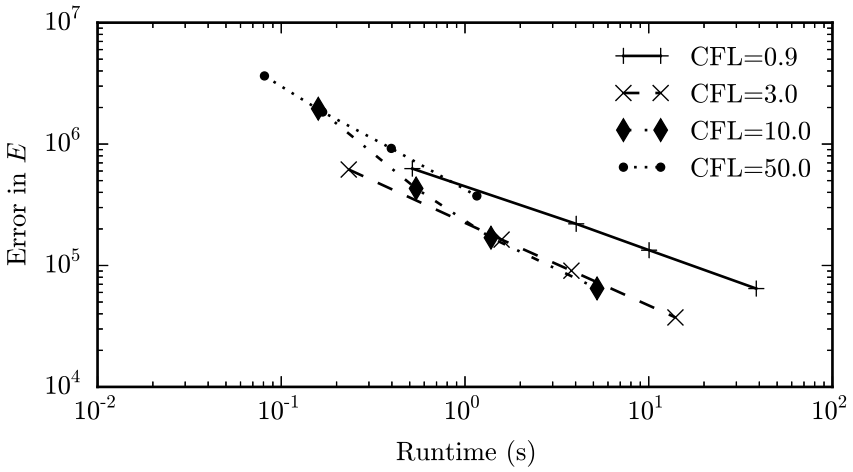

(c) Error in E.

Figure 4: Errors plotted against runtime for initial conditions given in eq. (17).

Figure 4 shows the error in the three conservative variables as function of runtime, for the four different Courant numbers considered. It is apparent that a Courant number of 3 gives a significantly lower error for a given runtime compared to $\mathcal{C} = 0.9$. This picture seems to be consistent for all the three conserved variables. Even $\mathcal{C} = 50.0$ achieves runtimes that are comparable to that of $\mathcal{C} = 0.9$ for a given error, although this requires a grid with about 7 times more cells.

4.3 Liquid-gas shock tube

In this case, the left part of the domain contains liquid at $60\,\mathrm{bar}$, whereas the right contains gas at $20\,\mathrm{bar}$. This is expected to be more challenging than the previous cases, since it requires handling both single-phase and two-phase regions. More precisely, the initial state is given by

$$u = 0, \tag{18a}$$

$$\alpha_\ell = \begin{cases} 1 & \text{if } x < 5000\,\mathrm{m}, \\ 0 & \text{if } x > 5000\,\mathrm{m}, \end{cases} \tag{18b}$$

$$p = \begin{cases} 60\,\mathrm{bar} & \text{if } x < 5000\,\mathrm{m}, \\ 20\,\mathrm{bar} & \text{if } x > 5000\,\mathrm{m}, \end{cases} \tag{18c}$$

$$T = T_{\mathrm{eq}}(p). \tag{18d}$$

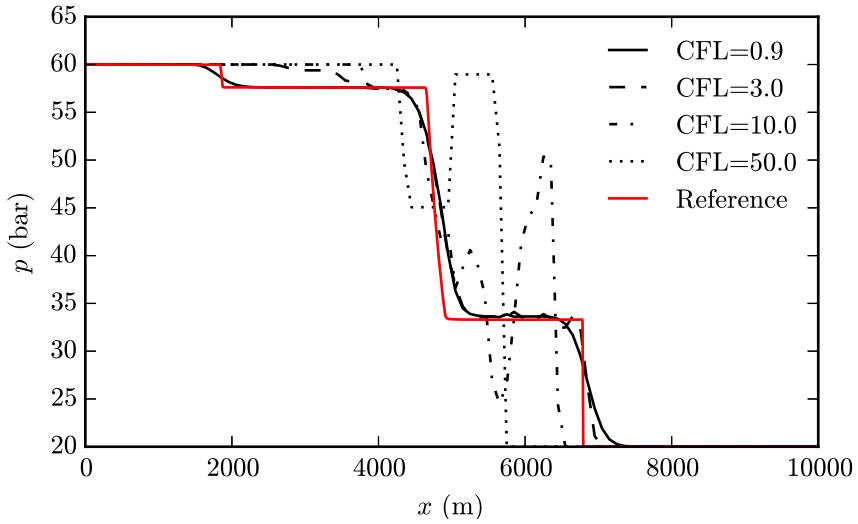

Figure 5: Pressure at time $t = 7\,\mathrm{s}$ on a grid with 100 cells for initial conditions given by eq. (18).

Figure 5 shows the pressure at $t = 7\,\mathrm{s}$ on a grid with 100 cells, compared to the reference solution. Both $\mathcal{C} = 10.0$ and $\mathcal{C} = 50.0$ lead to some significant oscillations, whereas $\mathcal{C} = 3.0$ performs quite well. However, it is apparent that the speed of the left-moving rarefaction wave (around $x = 2000\,\mathrm{m}$) is not resolved correctly and is notably different from the exact one.

Figure 6 shows the errors in the three conserved variables as function of runtimes. Also for this rather challenging case, the LTS Roe scheme outperforms the ordinary Roe scheme for moderate Courant numbers. Even a Courant number as high as 10 seems to be the best choice

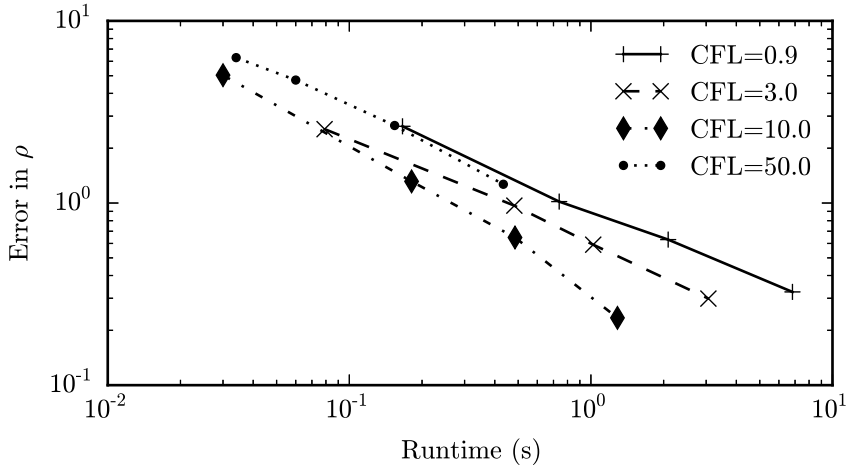

(a) Error in ρ.

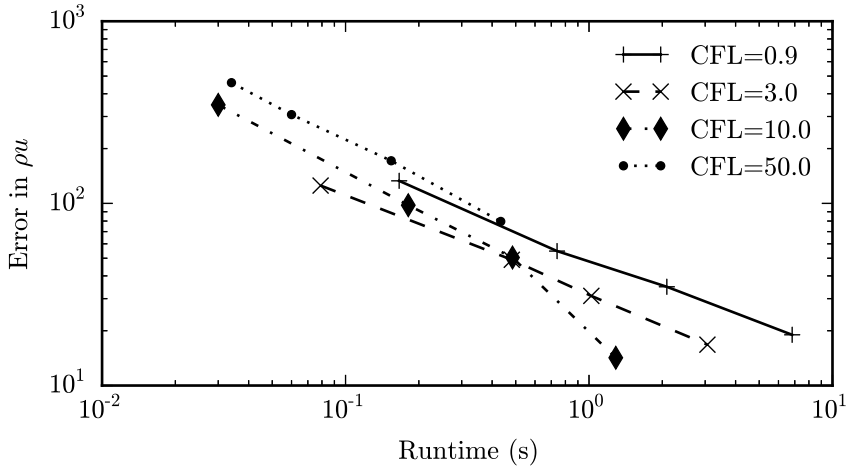

(b) Error in ρu.

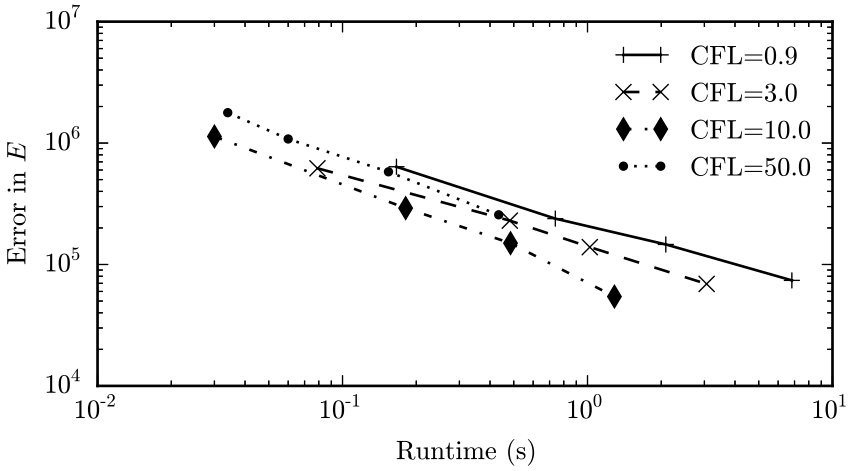

(c) Error in E.

Figure 6: Errors plotted against runtime for initial conditions given in eq. (18).

for this case when it comes to runtime, somewhat contrary to what one would expect when only considering fig. 5.

4.4 Smooth initial state

As a final test of how LTS Roe handles smoother initial states, we consider the following initial state:

$$\alpha_\ell = 0.6 \sin\left(\pi \frac{x}{10\,000\,\mathrm{m}}\right) + 0.2 \tag{19a}$$

$$u = \left(2.0 \cos\left(4\pi \frac{x}{10\,000\,\mathrm{m}}\right) + 2\right) \mathrm{m/s} \tag{19b}$$

$$p = \left(20 + \sin\left(1 + 4\frac{x}{10\,000\,\mathrm{m}}\right)\right) \mathrm{bar} \tag{19c}$$

$$T = T_{\mathrm{eq}}(p) \tag{19d}$$

Figure 7 shows the errors and runtimes for the three conserved variables. For this case, with rather smooth solutions, the LTS Roe scheme performs very well, and seems able to handle very large Courant numbers.

4.5 Discussion

From the results presented above, the main impression is that the LTS Roe scheme with moderate Courant numbers works well for a variety of different cases. For smooth solutions, very high Courant numbers can be tolerated and still produce results with a lower error-to-runtime ratio. The presence of shocks and strong nonlinearities seems to reduce the maximal suitable Courant number, which is to be expected since we assume all waves interact linearly. Nevertheless a Courant number of around 3 proved to be a good choice in all cases. Interestingly, this is very similar to what was reported by LeVeque [11] in his related scheme.

We have presented the dependence of the error on runtime and Courant number for the various cases. It is important to note that the time needed for different steps of the solution procedure might vary significantly depending on the application. In our case, a large portion of the simulation time is spent solving the two-phase equilibrium problem, mentioned in section 3. This makes it especially beneficial to increase the Courant number, since this leads to fewer executions of the two-phase equilibrium solver. The same considerations are likely to be relevant for other applications that involve computationally expensive thermodynamics.

Simply put, the solution procedure for a single time step consists of three parts:

1. Calculating the waves emanating from each cell interface by solving the Riemann problems,
2. propagating the waves over one or more cells (depending on the Courant number),
3. and projecting the resulting solution back onto the grid.

Each step involves a certain cost and introduces a certain error. In a typical application, step 1 incurs the highest costs, whereas steps 2 and 3 introduce the most errors. In step 2, the LTS Roe scheme is based on the assumption that the waves interact linearly, which leads to some errors. In addition, each projection in step 3 leads to projection errors. When increasing the

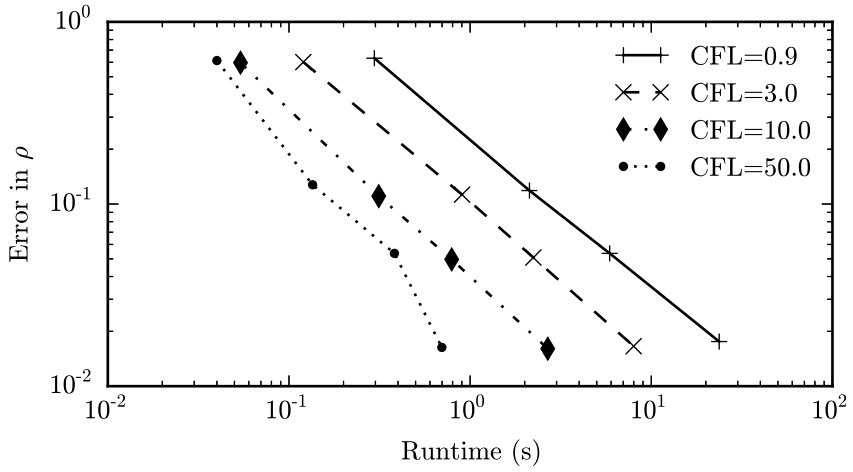

(a) Error in ρ.

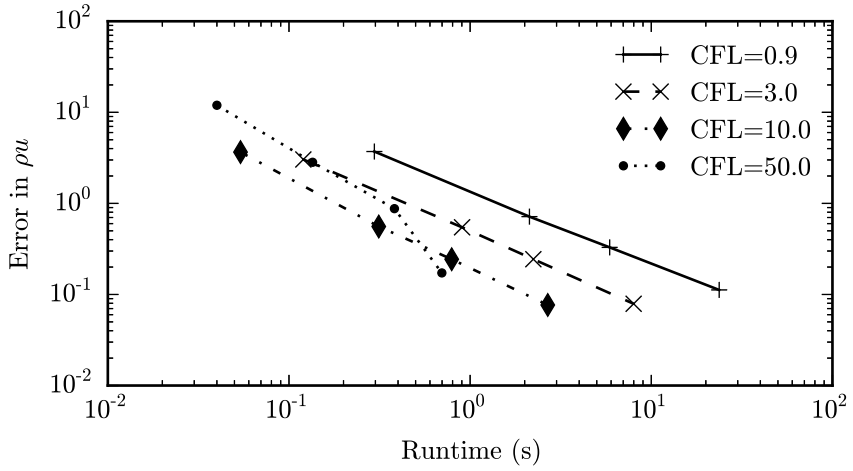

(b) Error in ρu.

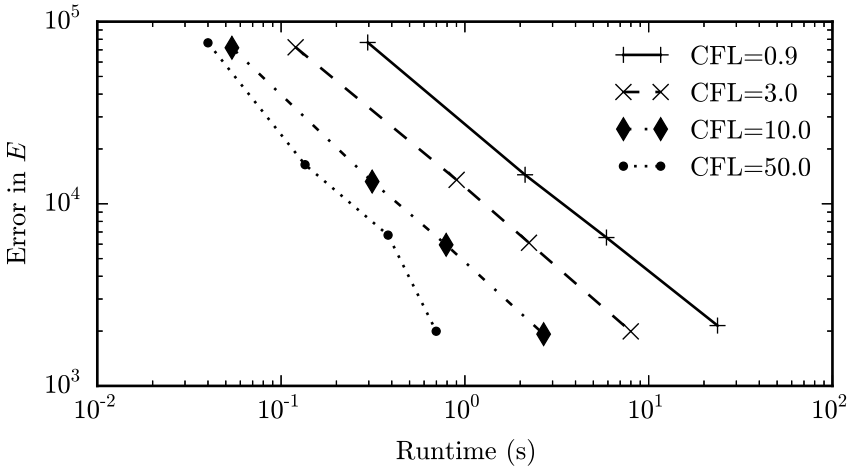

(c) Error in E.

Figure 7: Errors plotted against runtime for initial conditions given in eq. (19).

Courant number, we make a trade-off between increased error in step 2, reduced error (due to fewer executions) in step 3, and reduced cost (fewer executions) of step 1. The Courant number that gives the optimal trade-off (error versus runtime) will depend on the application.

5 SUMMARY

We have presented a two-phase flow model using the stiffened gas equation of state to describe the gas and liquid phases. The model was solved numerically with a novel large time step (LTS) Roe scheme. The LTS Roe scheme is based on the ordinary Roe scheme, but has a larger stencil which allows longer time steps while still being total-variation diminishing (TVD). Waves emanating from the Riemann problems are assumed to interact linearly, and propagated over one or more cells depending on the wave speed.

The LTS Roe scheme was applied to a number of test cases relevant to two-phase flow. It was shown that increasing the Courant number above 1 can give more accurate results for a certain runtime. For most cases, there is an optimal, finite Courant number that gives the optimal trade-off between runtime and error. Since the scheme is fully explicit, it is easily parallelizable, which is an advantage over implicit schemes.

As presented, the LTS Roe scheme is of first order, but we expect the scheme to be easily extendable to second order. Harten [4] expanded his similar scheme to second-order by applying to a modified flux using a minmod flux limiter. Furthermore, it is not straightforward to include source terms in a LTS scheme. A possibility is to use a fractional-step method such as Godunov or Strang splitting (see e.g. LeVeque [12, Ch. 17]), or to integrate the calculation of source terms directly with the wave propagation. This work verifies that the LTS Roe scheme, already successfully applied to shallow water flow [17, 19], aerodynamics [22] and Maxwell's equations [26], can be extended to more general equation systems.

Acknowledgements

This publication has been produced with support from the NORDICCS Centre, performed under the Top-level Research Initiative CO_2 Capture and Storage program, and Nordic Innovation. The authors acknowledge the following partners for their contributions: Statoil, Gassco, Norcem, Reykjavik Energy, and the Top-level Research Initiative (Project number 11029). The research has also received funding from the European Community's Seventh Framework Programme (FP7-ENERGY-20121-1-2STAGE) under grant agreement no. 308809 (The IMPACTS project). The authors acknowledge the project partners and the following funding partners for their contributions: Statoil Petroleum AS, Lundin Norway AS, Gas Natural Fenosa, MAN Diesel & Turbo SE and Vattenfall AB.

We would also like to thank our colleagues Peder Aursand, Tore Flåtten and Alexandre Morin for invaluable advice and discussions.

References

[1] S. Clerc. Numerical simulation of the homogeneous equilibrium model for two-phase flows. *Journal of Computational Physics*, 161(1):354–375, June 2000. doi: 10.1006/jcph.2000.6515.

[2] R. Courant, K. Friedrichs, and H. Lewy. On the partial difference equations of mathematical physics. *IBM Journal of Research and Development*, 11(2):215–234, 1967. doi: 10.1147/rd.112.0215.

[3] A. Harten. High resolution schemes for hyperbolic conservation laws. *Journal of Computational Physics*, 49(3):357–393, Mar. 1983. doi: 10.1016/0021-9991(83)90136-5.

[4] A. Harten. On a large time-step high resolution scheme. *Mathematics of Computation*, 46 (174):379–399, 1986. doi: 10.2307/2007983.

[5] A. Harten, J. M. Hyman, P. D. Lax, and B. Keyfitz. On finite-difference approximations and entropy conditions for shocks. *Communications on Pure and Applied Mathematics*, XXIX:297–322, 1976. doi: 10.1002/cpa.3160290305.

[6] H. Holden, K.-A. Lie, and N. H. Risebro. An unconditionally stable method for the Euler equations. *Journal of Computational Physics*, 150:76–96, 1999. doi: 10.1006/jcph.1998.6164.

[7] IEA. *Energy Technology Perspectives*. 2014. ISBN 978-92-64-20801-8. doi: 10.1787/energy_tech-2014-en.

[8] P. Lax and B. Wendroff. Systems of conservation laws. *Communications on Pure and Applied Mathematics*, 2:217–237, 1960. doi: 10.1002/cpa.3160130205.

[9] R. J. LeVeque. Large time step shock-capturing techniques for scalar conservation laws. *SIAM Journal on Numerical Analysis*, 19(6):1091–1109, 1982. doi: 10.1137/0719080.

[10] R. J. Leveque. Convergence of a large time step generalization of Godunov's method for conservation laws. *Communications on Pure and Applied Mathematics*, 37(4):463–477, 1984. ISSN 1097-0312. doi: 10.1002/cpa.3160370405.

[11] R. J. LeVeque. A large time step generalization of Godunov's method for systems of conservation laws. *SIAM Journal on Numerical Analysis*, 22(6):1051–1073, 1985. doi: 10.1137/0722063.

[12] R. J. LeVeque. *Finite Volume Methods for Hyperbolic Problems*. Cambridge University Press, New York, 2002.

[13] S. Lindqvist, P. Aursand, T. Flåtten, and A. A. Solberg. Large time step TVD schemes for hyperbolic conservation laws, 2015. URL `http://arxiv.org/abs/1511.07027`. Submitted.

[14] H. Lund, T. Flåtten, and S. T. Munkejord. Depressurization of carbon dioxide in pipelines – models and methods. In J. Gale, C. Hendriks, and W. Turkenberg, editors, *GHGT-10 – 10th International Conference on Greenhouse Gas Control Technologies*, pages 2984–2991, Amsterdam, The Netherlands, Sept. 2011. IEAGHGT, Energy Procedia vol. 4. doi: 10.1016/j.egypro.2011.02.208.

[15] R. Menikoff. Empirical equations of state for solids. *Shock Wave Science and Technology Reference Library*, 2:143–188, 2007.

[16] R. Menikoff and B. J. Plohr. The Riemann problem for fluid flow of real materials. *Review of Modern Physics*, 61(1):75–130, Jan.–Mar. 1989. doi: 10.1103/RevModPhys.61.75.

[17] M. Morales-Hernández, P. García-Navarro, and J. Murillo. A large time step 1D upwind explicit scheme (CFL $>$ 1): Application to shallow water equations. *J. Comput. Phys.*, 231(19):6532–6557, Aug. 2012. ISSN 0021-9991. doi: 10.1016/j.jcp.2012.06.017.

[18] A. Morin, P. K. Aursand, T. Flåtten, and S. T. Munkejord. Numerical resolution of CO_2 transport dynamics. In *SIAM Conference on Mathematics for Industry: Challenges and Frontiers (MI09)*, San Francisco, CA, USA, Oct. 2009.

[19] J. Murillo, P. García-Navarro, P. Brufau, and J. Burguete. Extension of an explicit finite volume method to large time steps (CFL $>$ 1): Application to shallow water flows. *International Journal for Numerical Methods in Fluids*, 50(1):63–102, 2006. ISSN 1097-0363. doi: 10.1002/fld.1036.

[20] M. R. Norman, R. D. Nair, and F. H. M. Semazzi. A low communication and large time step explicit finite-volume solver for non-hydrostatic atmospheric dynamics. *Journal of Computational Physics*, 230(4):1567–1584, 2011. ISSN 0021-9991. doi: 10.1016/j.jcp.2010.11.022.

[21] Z. Qian and C.-H. Lee. A class of large time step Godunov schemes for hyperbolic conservation laws and applications. *Journal of Computational Physics*, 230(19):7418 – 7440, 2011. doi: 10.1016/j.jcp.2011.06.008.

[22] Z. Qian and C.-H. Lee. On large time step TVD scheme for hyperbolic conservation laws and its efficiency evaluation. *Journal of Computational Physics*, 231:7415–7430, 2012. doi: 10.1016/j.jcp.2012.07.015.

[23] J.-M. Qui and C.-W. Shu. Convergence of Godunov-type schemes for scalar conservation laws under large time steps. *SIAM Journal on Numerical Analysis*, 46(5):2211–2237, 2007. doi: 10.2307/25663061.

[24] P. L. Roe. Approximate Riemann solvers, parameter vectors, and difference schemes. *Journal of Computational Physics*, 43(2):357–372, Oct. 1981. doi: 10.1016/0021-9991(81)90128-5.

[25] H. Städtke. *Gasdynamic aspects of two-phase flow*. Wiley-VCH, Weinheim, Germany, 2006. ISBN 3-527-40578-X.

[26] R. J. Thompson and T. Moeller. A discontinuous wave-in-cell numerical scheme for hyperbolic conservation laws. *Journal of Computational Physics*, 299:404–428, 2015. ISSN 0021-9991. doi: 10.1016/j.jcp.2015.06.047.

[27] H. C. Yee. Linearized form of implicit TVD schemes for the multidimensional Euler and Navier-Stokes equations. *Computers & Mathematics with Applications*, 12(4–5, Part A):413–432, 1986. ISSN 0898-1221. doi: 10.1016/0898-1221(86)90172-0.